Journal of Materials Chemistry C

ROYAL SOCIETY OF CHEMISTRY

PAPER

Cite this: J. Mater. Chem. C, 2021, 9, 16619

Predictable luminescence performance of polyphenylpyrazine derivatives based on a theoretical model *via* hole–electron overlap†

Juanjuan Luo,‡[a] Haozhong Wu,‡[a] Lu Liu,[a] Zhiming Wang *[a] and Ben Zhong Tang*[b]

Received 16th September 2021, Accepted 26th October 2021

DOI: 10.1039/d1tc04444c

rsc.li/materials-c

Tetraphenylpyrazine (TPP), as a multi-rotor type AIE building block with a better electron-withdrawing ability, has attracted much attention due to the unique photoelectric properties and wide applications of its derivatives. However, how to predict and amplify the AIE effect of its derivatives through structural control is an urgent problem to be solved. In this work, we develop a theoretical model for predicting the luminescence performance of TPP derivatives where the hole–electron overlap on the TPP unit is employed as a criterion with discussion based on in-depth theoretical calculations. The theoretical model indicates that the larger hole–electron overlap percentage on the TPP unit and the higher transition density matrix value of {TPP, TPP} will cause weaker emission in solution and a notable AIE process. Further expanding its universality to triphenylpyrazine-based derivatives, the experimental data and theoretical prediction are also very consistent, implying that this model based on hole–electron overlap could be expanded to more multi-rotor AIE luminogens.

1 Introduction

In the past few decades, organic luminescent materials have attracted tremendous interest especially in optoelectronic and biological fields.[1–4] However, most traditional luminescent materials often emit strongly in dilute solutions, but experience quenching in aggregation states which is known as the aggregation-caused quenching effect (ACQ).[5] This unsatisfactory phenomenon has limited the performance of luminescent materials in their practical application in aggregate forms. So, many efforts have been implemented to evade this adverse effect such as physical doping preparation in host materials and chemical modification strategy, but with finite effectiveness.[6–9]

In 2001, Tang's group proposed the opposite phenomenon, namely, aggregation-induced emission (AIE), in which some luminogens with a twisted conformation are weakly emissive in dilute solutions but the emission is enhanced in the aggregation state.[10] The intrinsic AIE feature equips AIE luminogens (AIEgens) with high photoluminescence quantum yield in the solid state and a microenvironment-sensitive fluorescence nature which furnish them with great potential applications in OLED and fluorescence sensing.[11–15] To explain the AIE phenomenon, some mechanisms have been put forward and proved theoretically and experimentally. Among them, restricted intramolecular rotation (RIR) has been widely recognized as one of the causes of AIE.[16–19]

TPP is a classical AIE luminophore dominated by the RIR mechanism, which exhibits the advantages of easy preparation and easy derivation.[20] Owing to the better electron-withdrawing ability of TPP, the donors usually are introduced to construct a D–A structure. TPP derivatives with D–A structures can possess many functionalities,[21–27] such as high charge transport ability, solvation response, and two-photon absorption which greatly broaden the application prospects of TPP derivatives in high-tech areas. However, when donors are introduced, the AIE performance of TPP derivatives may be weakened, which reduces the advantages of the AIE effect in application.[28] Therefore, it is necessary to study the method for predicting and amplifying the AIE effect of these D–A-type TPP derivatives through structural regulation and it is important to design AIE performance tailored materials.

In this work, theoretical methods are applied to discuss the AIE properties on TPP derivatives (**TPP-3C**, **TPP-TPA**, **PhCN-TPP-TPA**

[a] State Key Laboratory of Luminescent Materials and Devices, Center for Aggregation-Induced Emission, Key Laboratory of Luminescence from Molecular Aggregates of Guangdong Province, Guangzhou International Campus, South China University of Technology (SCUT), Guangzhou 510640, China. E-mail: wangzhiming@scut.edu.cn

[b] Shenzhen Institute of Aggregate Science and Technology, School of Science and Engineering, The Chinese University of Hong Kong, Shenzhen, Guangdong 518172, China. E-mail: tangbenz@cuhk.edu.cn

† Electronic supplementary information (ESI) available: Synthesis, characterization, and PL and UV spectra. See DOI: 10.1039/d1tc04444c

‡ These authors contributed equally to this work.

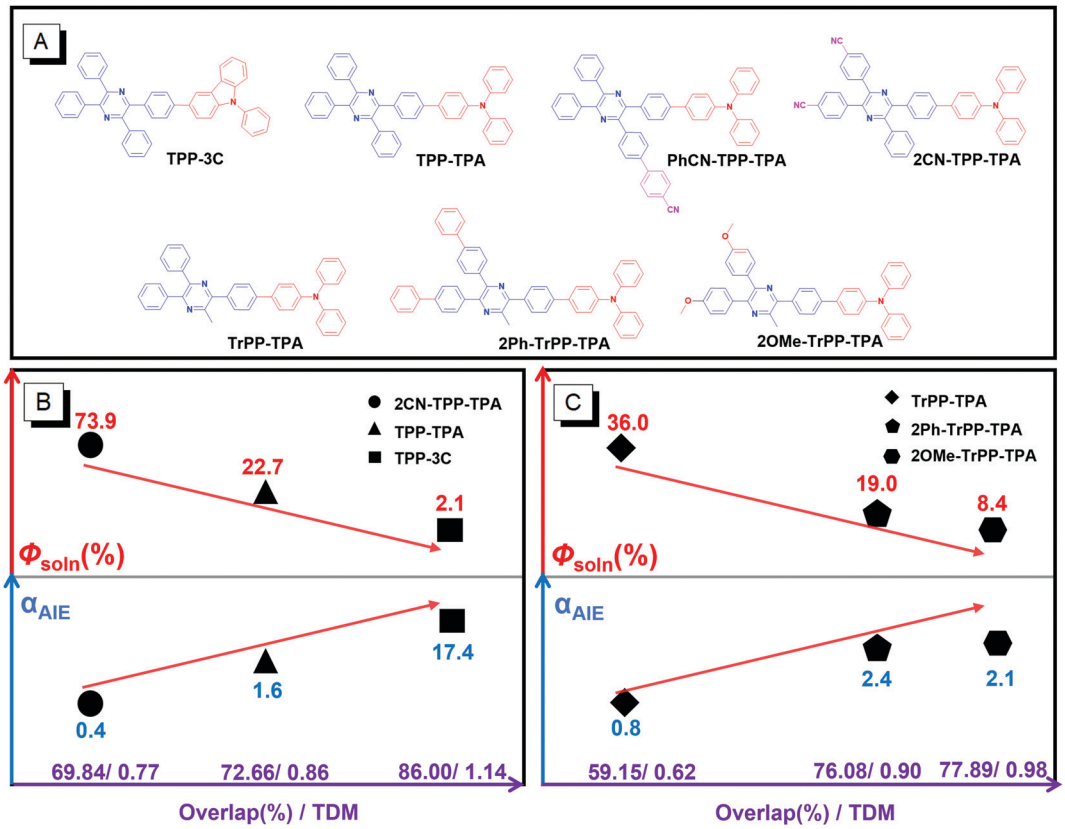

Scheme 1 (A) The molecule structures of TPP derivatives and TrPP derivatives. (B) The relationship between the luminescence performance and the value of hole-electron overlap on TPP and TDM of {TPP, TPP}. (C) The universality of the relationship on TrPP-based derivatives.

and **2CN-TPP-TPA**) where their hole–electron distribution is tuned by modifying the donors and acceptors (TPP analogues). The results indicate that the degree of hole–electron overlap on the TPP unit shows a remarkable influence on the luminescence performance. Therefore, we preliminarily propose a theoretical model for predicting the luminescence performance of TPP derivatives in which the hole–electron overlap percentage on the TPP unit and the transition density matrix (TDM) values of {TPP, TPP} are selected as parameters for prediction. The larger the values of the two parameters are, the weaker the emission in solution is and the better the AIE performance will be. Moreover, TrPP derivatives (**TrPP-TPA**, **2Ph-TrPP-TPA** and **2OMe-TrPP-TPA**) are synthesized for verifying the universality of the theoretical model (Scheme 1).

2 Results and discussion

2.1 Synthesis and characterization

The synthetic routes of these five compounds, **PhCN-TPP-TPA**, **2CN-TPP-TPA**, **TrPP-TPA**, **2Ph-TrPP-TPA**, and **2OMe-TrPP-TPA**, are outlined in Schemes S1 and S2 (ESI†). More detailed-synthetic procedures and characterization of the five target products are described in Fig. S1–S21 (ESI†). **PhCN-TPP-TPA** was obtained from the Schiff base cycling reaction of 1,2-diphenylethylenediamine and intermediate 5 in acetic acid. Mixing two benzoin derivatives (intermediate 2 and intermediate 4), ammonium acetate, and $CeCl_3{\cdot}7H_2O$ in ethanol, and refluxing the solution for 4 hours produced **2CN-TPP-TPA**. TrPP derivatives were produced by the Suzuki coupling reaction with the corresponding brominated intermediate and 4-(diphenylamino)phenylboronic acid. The products are soluble in common organic solvents, such as toluene, tetrahydrofuran (THF), and ethyl acetate, while not in water.

The photophysical properties of **TPP-3C** and **TPP-TPA** are obtained from a previous study.[26] The absorption and photoluminescence (PL) spectra of these newly synthesized five molecules were recorded under the same conditions and are depicted in Fig. S22–S33 (ESI†). All the photophysical data are summarized in Table 1.

2.2 Theoretical calculations on TPP-3C and TPP-TPA

The optimized S_0 and S_1 geometries were calculated using density functional theory (DFT) and time dependent density functional theory (TDDFT) respectively at the M062X/6-31G(d,p) level in the toluene phase *via* the Gaussian 16 package. More details about the theoretical methods are supplied in the ESI.† For exploring the influence of different donors on the AIE performance of TPP derivatives, theoretical calculations were employed separately in acceptor (TPP unit) and donor units (phenylcarbazole (3C), and triphenylamine (TPA)). As displayed in Fig. 1, TPA has a stronger electron donating ability than 3C according to previous reports,[26] so a higher energy of the

Table 1 The photophysical properties of TPP derivatives and TrPP derivatives

Molecules	λ_{abs}[a] [nm]	λ_{em}[b] [nm] Soln	Film	Φ[c] [%] Soln	Film	αAIE[d]	τ[e] [ns] Soln	Film
TPP-3C	350	441	447	2.1	36.6	17.4	0.51	0.91
TPP-TPA	364	458	468	22.7	35.2	1.6	0.55	0.91
PhCN-TPP-TPA	364	469	484	28.7	18.2	0.6	0.88	2.52
2CN-TPP-TPA	381	504	533	73.9	25.9	0.4	2.11	13.33
TrPP-TPA	357	442	467	36.0	30.3	0.8	0.68	1.34
2Ph-TrPP-TPA	360	449	474	19.0	44.8	2.4	0.49	0.99
2OMe-TrPP-TPA	361	431	464	8.4	17.5	2.1	0.63	1.01

[a] Absorptive peaks, concentration: 10×10^{-6} M. [b] Maximum emission wavelength, soln: toluene solution, film: neat film. [c] Absolute fluorescence quantum efficiency. [d] Φ_{film}/Φ_{soln}. [e] Fluorescence lifetime.

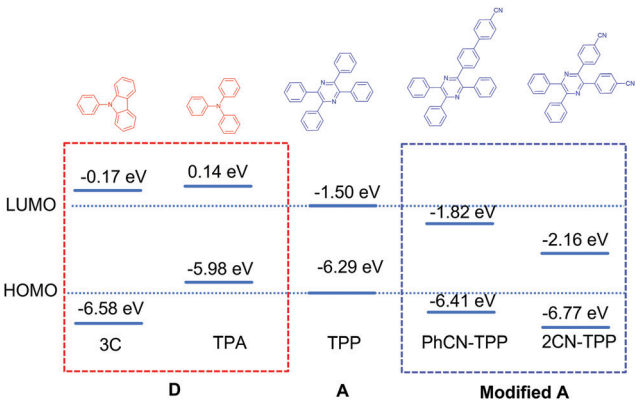

Fig. 1 HOMO and LUMO levels of TPP, 3C and TPA, PhCN–TPP and 2CN–TPP in the S_1 state by M062X/6-31G(d,p).

highest occupied molecular orbital (HOMO) is expected for TPA. Interestingly, the naked-TPP with a relatively high HOMO level (−6.29 eV) locates between those of naked-TPA (−5.98 eV) and naked-3C (−6.58 eV), but its lowest unoccupied molecular orbital (LUMO) level is much lower than naked-3C (−0.17 eV) and naked-TPA (0.14 eV), owing to the electron-withdrawing nature of pyrazine. Afterwards, the geometries of **TPP-3C** and **TPP-TPA** in the S_0 and S_1 states were optimized. Their HOMOs and LUMOs in the excited states are depicted in Fig. 2.

As shown in Fig. 2 and Table S1 (ESI†), the HOMO of **TPP-3C** mainly locates at the TPP unit and adjacent phenyl group (E) with an energy of −6.19 eV, close to that of naked-TPP (−6.29 eV). As for **TPP-TPA**, the HOMO mostly spreads on the TPA group, phenyl group (D), and pyrazine group (Py) with an energy of −5.94 eV, close to that of naked-TPA (−5.98 eV). Their LUMOs are majorly dispersed on the TPP unit with an energy of −1.69 eV and −1.46 eV, respectively. The results illustrate that the HOMOs of TPP-based derivatives would be more inclined to distribute on the units with higher HOMO levels, while LUMOs would tend to distribute on the unit with lower LUMO levels. Consequently, the less HOMO distribution on the TPP unit of **TPP-TPA** results in less HOMO–LUMO overlap on the TPP unit, compared to **TPP-3C**. The mentioned discipline of HOMO–LUMO distribution provides

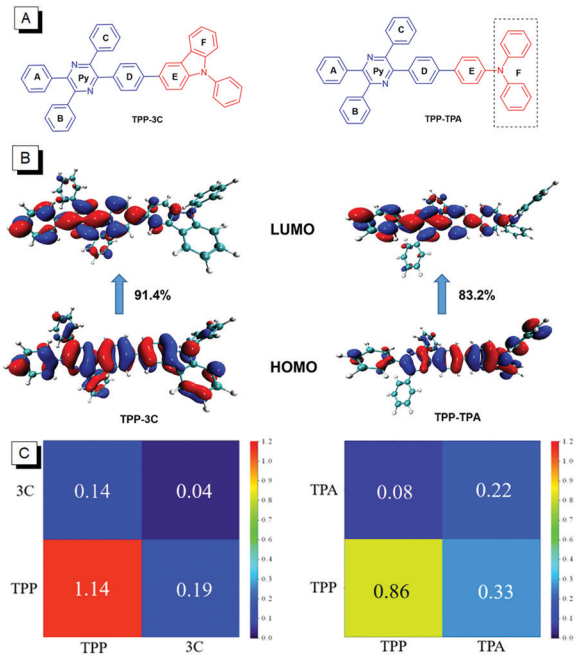

Fig. 2 The molecule structures (A), frontier orbital amplitude plot (B), and transition density matrices (C) of **TPP-3C** and **TPP-TPA** in the S_1 state by M062X/6-31G(d,p).

a strategy to tune the degree of HOMO–LUMO overlap on the TPP block by changing the relative HOMO level.

In addition, the natural transition orbitals (NTOs) are calculated to better understand their electronic structure. As displayed in Fig. S24 (ESI†), the NTO distributions are similar to the HOMO–LUMO distributions of **TPP-3C** and **TPP-TPA**, which are from their emission chiefly composed of the transition from the HOMO to LUMO, accounting for 91.4% of **TPP-3C** and 83.2% of **TPP-TPA** respectively. Meanwhile, the hole–electron distribution ratios on each unit are investigated to quantify the variation of distribution. As displayed in Table S2 (ESI†), both holes and electrons show large distribution percentages on the TPP unit of 83.76% and 88.30% in **TPP-3C**, so obvious hole–electron overlap with a degree of 86.00% occurs on the TPP unit. With respect to **TPP-TPA**, the percentage of holes on the TPP unit decreases to 64.23%, leading to less hole–electron overlap on TPP of 72.66%. Consistent with the frontier molecular orbital analysis, the stronger electron-donating group (TPA) could generate less hole–electron overlap on TPP. Generally, the less hole–electron overlap on TPP indicates a smaller influence of the TPP local excited state on the S_1–S_0 transition. Subsequently, the transition density matrices (TDM) of **TPP-3C** and **TPP-TPA** were calculated using the Multiwfn program for further clarifying the effect of each unit on the S_1–S_0 transition.

As displayed in Fig. 2C, the redshifted colour (value) of the blocks presents a positive correlation with the effect of each unit on the S_1–S_0 transition. The blocks such as {TPP, TPP} and {3C, 3C}, represent the local excited state (LE) component, while the other blocks, such as {3C, TPP} and {TPA, TPP} denote the charge transfer (CT) component. Obviously, in **TPP-3C**, the {TPP, TPP} block is the brightest with a value of

1.14 which demonstrates that the LE transition of TPP plays a key role in the whole transition process. However, the {TPP, TPP} block in TPP–TPA becomes blue-shifted with a decreased value of 0.86, while the value of {TPA, TPA} and {TPA, TPP} blocks increases to 0.22 and 0.33 of **TPP-TPA** from 0.04 and 0.19 of **TPP-3C**, respectively. Therefore, the local transition component of TPP becomes less predominant in the radiative transition of **TPP-TPA**, and the involvement of TPA turns out to be non-negligible which indicates the more extended hole–electron distribution. According to the previous study of TPP, TPP exhibits a faint emission in solution due to the rotation of peripheral-phenyl groups which can be restricted by aggregation and prompt AIE features.[20] Therefore, the less local transition component on the TPP unit can weaken the effect from the rotation of peripheral-phenyl groups in the transition process in **TPP-TPA**, so that a strong emission in solution and a weak AIE phenomenon could be observed. Consistent with the theoretical analysis, **TPP-3C** shows a very obvious AIE phenomenon where the corresponding fluorescence quantum efficiencies (Φs) are 2.1% and 36.6% respectively in toluene and film states, while **TPP-TPA** displays a weak AIE phenomenon with Φ of 22.7% in toluene and 35.2% in film states (Table 1).[26]

As analysis thereinbefore, the AIE process shows a positive correlation with the degree of hole–electron overlap on the TPP unit, while the emission intensity in solution shows a contrary correlation. The donor with a lower HOMO energy level will increase the degree of hole–electron overlap on the TPP unit which causes a weak emission in solution and a stronger AIE performance. Accordingly, we put forward a theoretical model where the theoretical calculations are employed for predicting the luminescence performance: the larger the values of hole–electron overlap percentage on the TPP unit and the TDM value of {TPP, TPP} are, the weaker the emission in solution is and the stronger the AIE phenomenon of TPP-based derivatives will be.

2.3 Theoretical model verification in TPA-substituted TPP derivatives

2.3.1 Theoretical calculations. To further verify the feasibility of the theoretical model, another two acceptor modified TPP derivatives were synthesized by introducing 4-cyanobenzene (PhCN) and cyanogroup (2CN) on the TPP group. The same theoretical calculations were employed on the modified-TPP group (including the PhCN–TPP group and 2CN–TPP group), **PhCN-TPP-TPA** and **2CN-TPP-TPA.** As illustrated in Fig. 1 and Table S3 (ESI†), the HOMO levels of the PhCN–TPP group and 2CN–TPP group fall to −6.41 eV and −6.77 eV lower than −6.29 eV of naked-TPP, on account of introducing the electron-withdrawing group. As depicted in Fig. 3, the HOMO of **PhCN-TPP-TPA** principally locates on the TPA group, phenyl groups (D), and pyrazine, while the LUMO is mainly dispersed on the TPP group similarly to **TPP-TPA**. With respect to **2CN-TPP-TPA**, the

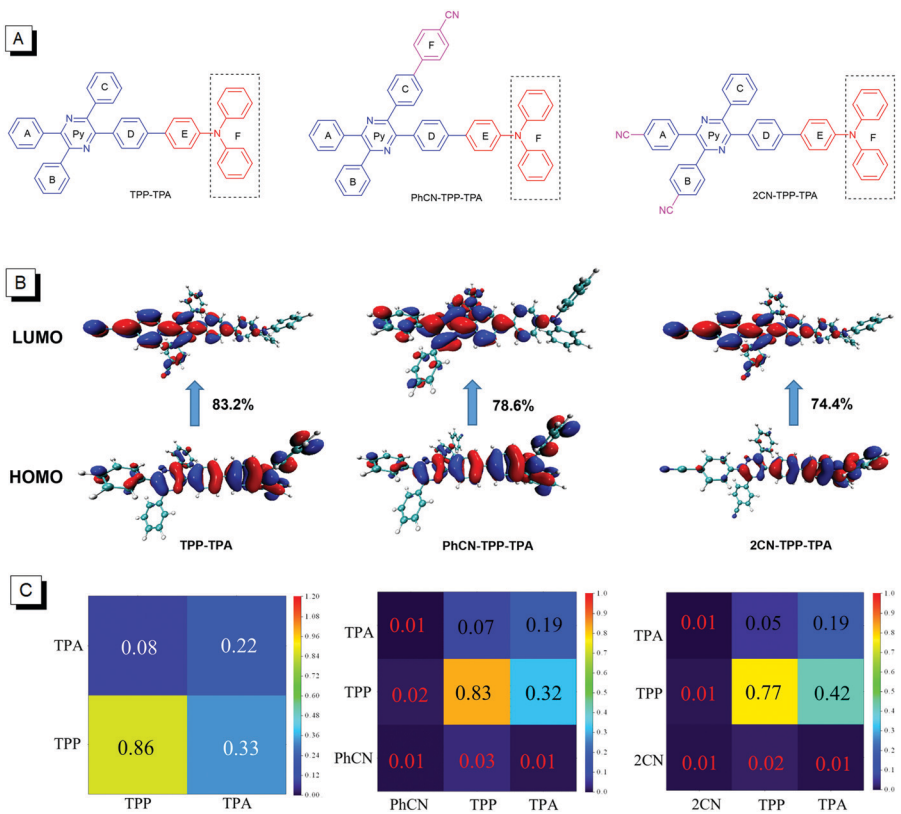

Fig. 3 The molecular structures (A), frontier orbital amplitude plot (B) and transition density matrices (C) of **TPP-TPA**, **PhCN-TPP-TPA** and **2CN-TPP-TPA** in the S_1 state by M062X/6-31G(d,p).

HOMO on the pyrazine unit apparently reduces, and the LUMO mainly centers on the TPP group. Therefore, the HOMO–LUMO overlap on the TPP unit of **2CN-TPP-TPA** is the least among the three TPA-substituted derivatives. Their hole–electron distributions are consistent with the HOMO–LUMO distributions (Fig. S24, ESI†). The result preliminary indicates that lowering the HOMO level of naked-TPP by modification of the TPP group with strong electron-withdrawing groups can decrease the hole–electron overlap on the TPP unit.

To predict the luminescence properties of these two molecules, their percentages of hole–electron overlap on TPP and TDM values of the {TPP, TPP} block were calculated by identical theoretical methods. The percentage of holes on the TPP unit is 64.84% for **PhCN-TPP-TPA,** similar to 64.23% of TPP–TPA, while it reduces to 57.91% for **2CN-TPP-TPA**. Thus, the least hole–electron overlap on the TPP appears for **2CN-TPP-TPA** with a percentage of 69.84% (Table S4, ESI†). The TDM values of the {TPP, TPP} blocks are 0.86, 0.83 and 0.77 respectively for **TPP-TPA**, **PhCN-TPP-TPA**, and **2CN-TPP-TPA**. In addition, the {TPA, TPP} block becomes brighter with a value of 0.42 in **2CN-TPP-TPA,** indicating more extended conjugation and CT components (Fig. 3C). According to the theoretical model, **PhCN-TPP-TPA** should have similar luminescence properties to TPP–TPA. With the smallest percentage of hole–electron overlap on TPP and TDM value of the {TPP, TPP} block, **2CN-TPP-TPA** should have the strongest emission in solution and least obvious AIE phenomenon among the three TPA-substituted TPP derivatives.

2.3.2 Photophysical data. The photophysical properties are analysed using the absorption and PL spectrum for confirming the above speculation. **PhCN-TPP-TPA** and **2CN-TPP-TPA** exhibit strong absorption bands around 350–400 nm (Fig. S22, ESI†). Consistent with the theoretical prediction, **PhCN-TPP-TPA** (Φ_{soln}: 28.7%) and **TPP-TPA** (Φ_{soln}: 22.7%) show similar luminescence properties in solution. But **PhCN-TPP-TPA** with ortho substitutions of PhCN and TPA might pack loosely and quench in the aggregate state which causes unexpectedly lower α_{AIE} than TPP–TPA.[25] It is noteworthy that the Φ of **2CN-TPP-TPA** (73.9%) is much higher than that of **TPP-TPA** (22.7%) and **PhCN-TPP-TPA** (28.7%) in toluene. Moreover, the smallest α_{AIE} (0.4) for **2CN-TPP-TPA** manifests that **2CN-TPP-TPA** shows the weakest AIE phenomenon among the three TPA-substituted compounds consistent with theoretical speculation (Table 1).

The results show the feasibility of the theoretical model which can predict accurate luminescence properties in solution and an approximate trend of AIE performance (α_{AIE}). In addition, the lower HOMO level of the modified TPP group with a strong electron-withdrawing nature will decrease the hole–electron overlap on the TPP unit, leading to better emission in solution and weaker AIE performance. These results provide a method for regulating the luminescence performance of TPP derivatives by tuning the relative HOMO level of the TPP unit.

2.4 Universal expansion in triphenylpyrazine derivatives (TrPP)

The TrPP derivative is a newly developed polyphenylpyrazine derivative with AIE properties which shows great potential in non-doped OLEDs owing to its high photoluminescence efficiency and deep-blue emission.[27] TrPP is also an electron deficient material with a multi-rotor configuration which is similar to TPP. Therefore, the above theoretical model for predicting the luminescence performance might be applicable for TrPP derivatives. For proving the universality of the theoretical model on polyphenylpyrazine derivatives, we designed three molecules, **TrPP-TPA**, **2Ph-TrPP-TPA** and **2OMe-TrPP-TPA**.

2.4.1 Theoretical calculations. As expected, the HOMO levels of the 2Ph–TrPP group and 2OMe–TrPP group are increased to −6.26 eV, and −6.04 eV compared with that of the naked-TrPP (−6.35 eV) because of the increased conjugation and the introduction of electron-donating methoxy on the TrPP group (Fig. 4 and Table S5, ESI†). Naked-TrPP and the modified-TrPP group (including the 2Ph–TrPP group and 2OMe–TrPP) have a much lower LUMO level than naked-TPA, so the LUMOs of **TrPP-TPA**, **2Ph-TrPP-TPA** and **2OMe-TrPP-TPP** show little difference mainly located on the TrPP unit. The HOMO of **TrPP-TPA** majorly locates on the TPA group, phenyl group (D), pyrazine, and little spread on the phenyl group (A). It is noteworthy that the HOMO distribution on the phenyl group (A) of **2Ph-TrPP-TPA** and **2OMe-TrPP-TPP** gradually increases indicating the increment of the HOMO–LUMO overlap on the TrPP unit (Fig. 5B). The hole–electron distributions are basically the same as HOMO–LUMO distributions (Fig. S24, ESI†). These results illustrate that introducing benzene and methoxy on the TrPP group would improve the HOMO level of TrPP and produce more hole–electron overlap on the TrPP block.

As shown in Table S6 (ESI†), the percentage of holes on the TrPP group is 48.74% in **TrPP-TPA**, while it ascends to 69.07% and 71.91% respectively for **2Ph-TrPP-TPA** and **2OMe-TrPP-TPA**. The percentages of electrons on the TrPP group in these three molecules are approximate. So, the percentages of hole–electron overlap on the TrPP group gradually improve in the order of **TrPP-TPA** (59.15%), **2Ph-TrPP-TPA** (76.08%) and **2OMe-TrPP-TPA** (77.89%). As shown in the transition density matrices (Fig. 5C), the values of the {TrPP, TrPP} block gradually increase in the

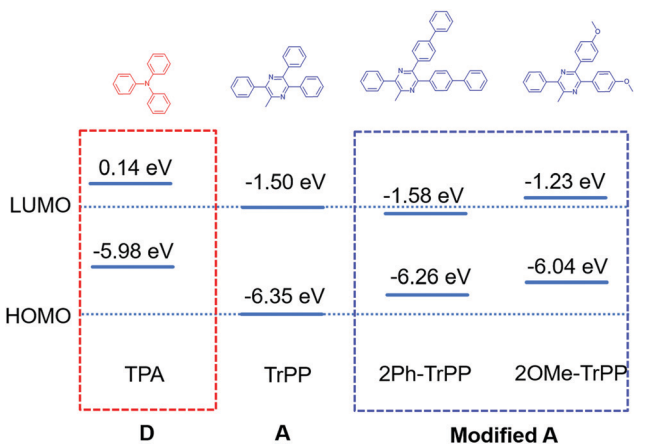

Fig. 4 HOMO and LUMO levels of TPA, TrPP, 2Ph–TrPP, and 2OMe–TrPP in the S_1 state by M062X/6-31G(d,p).

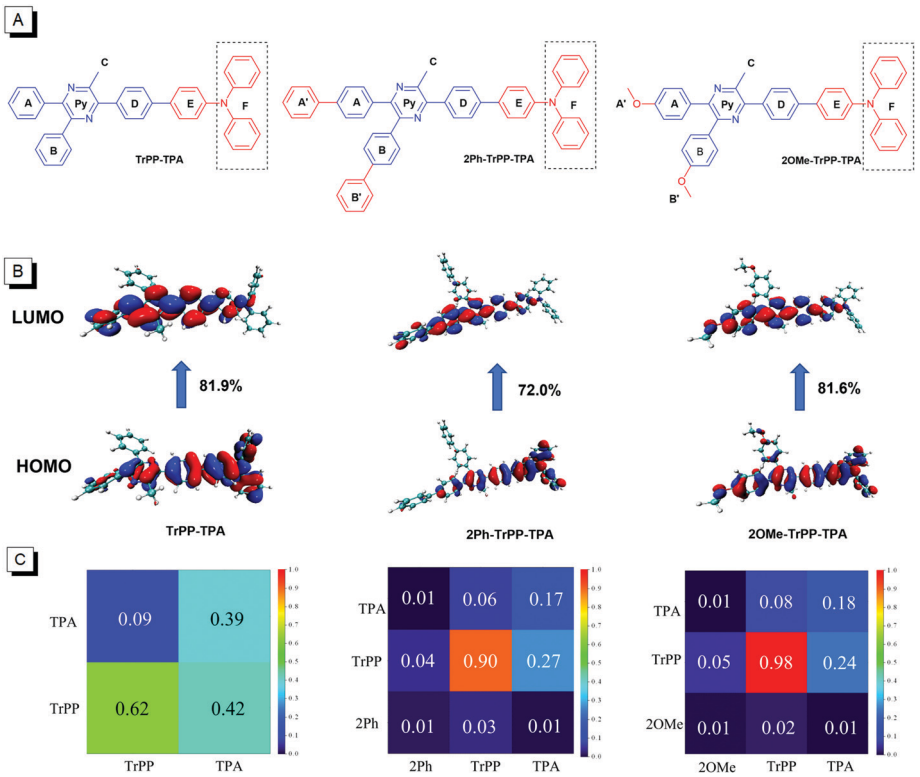

Fig. 5 The molecular structures (A), frontier orbital amplitude plot (B) and transition density matrices (C) of TrPP derivatives in the S_1 state by M062X/6-31G(d,p).

order of **TrPP-TPA** (0.62), **2Ph-TrPP-TPA** (0.90), and **2OMe-TrPP-TPA** (0.98). This implies that the local transition of the TrPP group becomes more dominant in the radiative process after introducing benzene and methoxy on the TrPP unit. Based on the theoretical model, **2Ph-TrPP-TPA** and **2OMe-TrPP-TPA** should have weaker emission in solution and exhibit a more obvious AIE phenomenon than **TrPP-TPA.**

2.4.2 Photophysical data. These three molecules (**TrPP-TPA**, **2Ph-TrPP-TPA**, and **2OMe-TrPP-TPA**) exhibit strong absorption bands around 320–400 nm in toluene solution belonging to the π–π* transition of conjugated molecular backbones (Fig. S23, ESI†). The emission peaks of them locate at 431–474 nm in toluene and film states. Their emission intensity in solution gradually decreases in the order of **TrPP-TPA** (36.0%), **2Ph-TrPP-TPA** (19.0%) and **2OMe-TrPP-TPA** (8.4%) in line with the theoretical model. Moreover, **2Ph-TrPP-TPA** and **2OMe-TrPP-TPA** show a stronger AIE phenomenon with α_{AIE} values of 2.4 and 2.1 respectively compared with **TrPP-TPA** (α_{AIE}: 0.8) consistent with the theoretical prediction. **2OMe-TrPP-TPA** shows a lower α_{AIE} than **2Ph-TrPP-TPA** which might come from the different packing ways in the solid state influenced by substituting the non-planar methoxy group. (Table 1) This theoretical model predicts the accurate emission intensity of the three molecules in solution and the approximate trend of AIE performance. These results demonstrate the universality of the theoretical model on polyphenylpyrazine derivatives. Furthermore, **2Ph-TrPP-TPA** and **2OMe-TrPP-TPA** exhibit better AIE performance by improving the HOMO level of the modified-TrPP group which also indicates the feasibility of the method for regulating the AIE performance.

3 Conclusions

Based on the theoretical analysis on the AIE properties of **TPP-3C** and **TPP-TPA**, we propose a theoretical model *via* hole–electron overlap for predicting the luminescence performance of TPP-based derivatives. The percentage of hole–electron overlap on the TPP unit and TDM value of {TPP, TPP} are selected as prediction parameters. The larger the value of them is, the weaker the emission in solution is and the more obvious the AIE phenomenon of TPP derivatives will be. The theoretical model successfully predicts the luminescence performance of TPP- and TrPP-based derivatives, which all prove the universality of this theoretical model. Therefore, we believe that this model could be applied to more multi-rotor type AIE building blocks. In addition, this research inspires us to obtain AIE tailored materials by tuning the relative HOMO level between the electron-withdrawing AIE block and the donor.

Author contributions

Juanjuan Luo: methodology, investigation, visualization, and writing – original draft. Haozhong Wu: methodology, formal analysis, investigation, and writing – review & editing. Lu Liu:

writing – review & editing. Zhiming Wang: supervision, and writing – review & editing. Benzhong Tang: supervision.

Conflicts of interest

There are no conflicts to declare.

Acknowledgements

This work is financially supported by the National Natural Science Foundation of China (21788102 and 21975077), the National Key R&D Program of China (Intergovernmental cooperation project, 2017YFE0132200), the Open Research Project of Military Logistics Support Department (BLB19J008), the Fundamental Research Funds for the Central Universities (2019ZD04), the Natural Science Foundation of Guangdong Province (2020A1515011542) and the Fund of Guangdong Provincial Key Laboratory of Luminescence from Molecular Aggregates (2019B030301003)

Notes and references

1 Y. Xu, X. Liang, X. Zhou, P. Yuan, J. Zhou, C. Wang, B. Li, D. Hu, X. Qiao, X. Jiang, L. Liu, S. J. Su, D. Ma and Y. Ma, *Adv. Mater.*, 2019, **31**, 1807388.

2 X. Ai, E. W. Evans, S. Dong, A. J. Gillett, H. Guo, Y. Chen, T. J. H. Hele, R. H. Friend and F. Li, *Nature*, 2018, **563**, 536–540.

3 Q. Wan, R. Zhang, Z. Zhuang, Y. Li, Y. Huang, Z. Wang, W. Zhang, J. Hou and B. Z. Tang, *Adv. Funct. Mater.*, 2020, **30**, 2002057.

4 H. Li, H. Kim, J. Han, V. Nguyen, X. Peng and J. Yoon, *Aggregate*, 2021, **2**, 1–30.

5 J. B. Birks, *Photophysics of aromatic molecules*, Wiley, London, 1970.

6 Z. Li, B. Jiao, Z. Wu, P. Liu, L. Ma, X. Lei, D. Wang, G. Zhou, H. Hu and X. Hou, *J. Mater. Chem. C*, 2013, **1**, 2183–2192.

7 J. Y. Hu, Y. J. Pu, F. Satoh, S. Kawata, H. Katagiri, H. Sasabe and J. Kido, *Adv. Funct. Mater.*, 2014, **24**, 2064–2071.

8 S. Wang, M. Qiao, Z. Ye, D. Dou, M. Chen, Y. Peng, Y. Shi, X. Yang, L. Cui, J. Li, C. Li, B. Wei and W. Y. Wong, *iScience*, 2018, **9**, 532–541.

9 S. A. Swanson, G. M. Wallraff, J. P. Chen, W. Zhang, L. D. Bozano, K. R. Carter, J. R. Salem, R. Villa and J. C. Scott, *Chem. Mater.*, 2003, **15**, 2305–2312.

10 J. Luo, Z. Xie, Z. Xie, J. W. Y. Lam, L. Cheng, H. Chen, C. Qiu, H. S. Kwok, X. Zhan, Y. Liu, D. Zhu and B. Z. Tang, *Chem. Commun.*, 2001, 1740–1741.

11 H. Zhang, J. Zeng, W. Luo, H. Wu, C. Zeng, K. Zhang, W. Feng, Z. Wang, Z. Zhao and B. Z. Tang, *J. Mater. Chem. C*, 2019, **7**, 6359–6368.

12 J. Huang, H. Nie, J. Zeng, Z. Zhuang, S. Gan, Y. Cai, J. Guo, S. J. Su, Z. Zhao and B. Z. Tang, *Angew. Chem., Int. Ed.*, 2017, **56**, 12971–12976.

13 J. Liang, R. T. K. Kwok, H. Shi, B. Z. Tang and B. Liu, *ACS Appl. Mater. Interfaces*, 2013, **5**, 8784–8789.

14 R. Nazarian, H. R. Darabi, K. Aghapoor, R. Firouzi and H. Sayahi, *Chem. Commun.*, 2020, **56**, 8992–8995.

15 A. C. Sedgwick, L. Wu, H. H. Han, S. D. Bull, X. P. He, T. D. James, J. L. Sessler, B. Z. Tang, H. Tian and J. Yoon, *Chem. Soc. Rev.*, 2018, **47**, 8842–8880.

16 J. Zhang, H. Zhang, J. W. Y. Lam and B. Z. Tang, *Chem. Res. Chin. Univ.*, 2021, **37**, 1–15.

17 Q. Peng and Z. Shuai, *Aggregate*, 2021, **e91**, 1–20.

18 N. L. C. Leung, N. Xie, W. Yuan, Y. Liu, Q. Wu, Q. Peng, Q. Miao, J. W. Y. Lam and B. Z. Tang, *Chem. – Eur. J.*, 2014, **20**, 15349–15353.

19 Y. Hong, J. W. Y. Lam and B. Z. Tang, *Chem. Commun.*, 2009, 4332–4353.

20 M. Chen, L. Li, H. Nie, J. Tong, L. Yan, B. Xu, J. Z. Sun, W. Tian, Z. Zhao, A. Qin and B. Z. Tang, *Chem. Sci.*, 2015, **6**, 1932–1937.

21 H. Wu, X. Song, B. Zhang, Z. Wang, T. Zhang, A. Qin and B. Z. Tang, *Mater. Chem. Front.*, 2020, **4**, 1706–1713.

22 B. Zhang, H. Wu, Z. Wang, A. Qin and B. Z. Tang, *J. Mater. Chem. C*, 2020, **8**, 4754–4762.

23 H. Wu, Y. Pan, J. Zeng, L. Du, W. Luo, H. Zhang, K. Xue, P. Chen, D. L. Phillips, Z. Wang, A. Qin and B. Z. Tang, *Adv. Opt. Mater.*, 2019, **7**, 1900283.

24 M. Chen, H. Nie, B. Song, L. Li, J. Z. Sun, A. Qin and B. Z. Tang, *J. Mater. Chem. C*, 2016, **4**, 2901–2908.

25 L. Pan, H. Wu, J. Liu, K. Xue, W. Luo, P. Chen, Z. Wang, A. Qin and B. Z. Tang, *Adv. Opt. Mater.*, 2019, **7**, 1801673.

26 H. Wu, J. Luo, Z. Xu, Z. Wang, D. Ma, A. Qin and B. Z. Tang, *Chem. Res. Chin. Univ.*, 2020, **36**, 61–67.

27 H. Wu, J. Zeng, Z. Xu, B. Zhang, H. Zhang, Y. Pan, Z. Wang, D. Ma, A. Qin and B. Z. Tang, *J. Mater. Chem. C*, 2019, **7**, 13047–13051.

28 H. Wu, G. Li, J. Luo, T. Chen, Y. Ma, Z. Wang, A. Qin and B. Z. Tang, *Adv. Opt. Mater.*, 2021, 2101085.